PROCEEDINGS OF SCIENCE

ONLINE ICRC 2021
THE ASTROPARTICLE PHYSICS CONFERENCE
Berlin | Germany
37th International Cosmic Ray Conference
12–23 July 2021

Fast X-ray variability of radio galaxy M87

Ryo Imazawa,[a,*] **Yasushi Fukazawa,**[a] **Hiromitsu Takahashi**[a] **and Mahito Sasada**[b]

[a] *Hiroshima University Graduate School of Advanced Science and Engineering, 1-3-1 Kagamiyama, Higashi-Hiroshima, Hiroshima 739-8526, Japan*

[b] *Hiroshima University, Hiroshima Astrophysical Science Center, 1-3-1 Kagamiyama, Higashi-Hiroshima, Hiroshima 739-8526, Japan*

E-mail: imazawa@astro.hiroshima-u.ac.jp

M87 is one of the nearest radio galaxy. We can study the core, jet, and some components by radio to X-ray observations. Regarding TeV gamma ray observations, it is known to show an intra-day variability. Such fast variability may occur at the particle acceleration region. But due to rough angular resolution, we cannot know which component causes this variability. We searched for short term X-ray variability of the M87 from long-exposure X-ray archive data. As a result, we found an intra-day variability during Suzaku/XIS data in 2006. Suzaku/XIS cannot resolve each component, but HST-1 was the brightest component in the X-ray band in this period; core had 1/4 of HST-1 flux. Therefore, this variability possibly comes from HST-1, but we cannot rule out the possibility of large core variability. A soft photon index of 2.08 in the X-ray band indicates that variability component is synchrotron emission from accelerated electrons in HST-1 or core.
In addition, we also find a possible variability of core on the Chandra/HRC observation in 2017. In this period, NuStar X-ray spectra have a power law with a photon index of 1.8, and thus not likely a synchrotron spectrum from the jet. Here the X-ray emission from the core was dominant in this period. Also, we find that one NuStar observation showed a higher flux than other NuStar observations by a factor of 2.5.

From these results, both core and HST-1 can be the origin of the X-ray variability. We will discuss the variability site and emission mechanism.

37th International Cosmic Ray Conference (ICRC 2021)
July 12th – 23rd, 2021
Online – Berlin, Germany

*Presenter

1. Introduction

Radio galaxy is one type of Active Galactic Nuclei (AGN), which has strong jet and large inclination. Some radio galaxies were detected by TeV gamma-ray observations, M87 is one of it. M87 is a nearby FR-I radio galaxy as redshift z = 0.0042 (∼16 Mpc). Its jet components have been resolved through radio, optical, and X-ray observations. Thus, it is good sample to study morphology study, thus many observations by each wavelength were performed. TeV gamma-ray from M87 was detected by MAGIC and H.E.S.S., and they found daily scale variability. It indicates particle acceleration in the jet, but location of this is still under debate.

In this study, we studied X-ray fast variability of M87 to study the location of the source of particle acceleration. In Section 2, we describe observations and data analysis. In Section 3, we describe the results of time variability and spectral analysis. Finally, in Section 4, we discuss the origin of intraday X-ray time variability.

2. Observation and Analysis

We chose X-ray data that have a longer exposure time of more than 10ksec to search for X-ray intraday variability. For Chandra data, we chose data taken directly by Advanced CCD Imaging Spectrometer (ACIS) and High Resolution Camera (HRC); imaging observations without grating. For ACIS data, we chose data taken with a shortframe time of 0.4 sec (sub-array mode) to minimize pile up effects. As a result, 15 Chandra data (13 ACIS and 2 HRC), 6 NuSTAR data, and 1 Suzaku data were found. There are 6 NuSTAR observations with more than 10 ksec, andChandra observed simultaneously with each NuSTAR observation. Since NuSTAR cannot resolve each jet component,Chandra data was useful and thus these data are analyzed, even though their exposure time is short. Table 1, 2, and 3 summarize the list of observation data analyzed in this article.

2.1 Light curve

To study a short-term variability, we derived an X-ray light curve in each observation. For Chandra, we derived light curves of each component in the jet: core, HST-1, knot D, and knot A. The extraction region of each component is shown in Figure 2. The position at 0.8 arcsec from the core is defined as HST-1. In addition, knots D and A are defined in order from the core, and their positions are set at 2.9 and 12.4 arcsec from the core, respectively. Chandra light curves were created by the `dmextract` command in `CIAO` in the energy range of 2.0–10.0 keV (HRC data was not filtered) with a time bin of 3600 ksec. To evaluate the variability of the background signal, light curves of the background region are created in the same way to source light curves, but the position is at 5.0 arcsec from the core in the direction opposite to the jet.

For NuSTAR, we derived light curves of FPMA and FPMB separately in each observation. The source area is defined as a circle with a radius of 30 arcsec. A light curve was created with the `lcurve` command in an energy range of 8.0–30.0 keV with a time bin of 3600 s. As shown in §2.2.1, the AGN emission is dominant above 8.0 keV. Light curves of the background region were made with the same radius as the source region at 3.2 arcmin from M87.

The Suzaku satellite observed M87 for two days from November 29 to December 1, 2006 (MJD: 54068-54070). In this study, we used data obtained via X-ray Imaging Spectrometer (XIS).

Table 1: List of Chandra data analyzed in this paper. ID:13515 and ID:18612 were taken by HRC, marked with asterisk to the right of Obs ID. Others data were taken by ACIS. Results of the short-term variability study are also presented as root mean square (RMS) (see Section 3). "-" means that variability was insignificant.

Start date (YYYY-MM-DD)	Obs ID	exposure time (ksec)	RMS	RMS_{bgd}
2012-04-14	13515*	74.3	-	-
2016-02-23	18233	37.2	0.04±0.02 (core)	-
2016-02-24	18781	39.5	-	-
2016-02-26	18782	34.1	-	-
2016-04-20	18783	36.1	0.05±0.03 (core)	0.22±0.09
2016-04-28	18836	38.9	-	-
2016-05-28	18838	56.3	0.06±0.02 (knot A)	-
2016-06-12	18856	25.5	-	-
2017-02-15	19457	4.6	-	-
2017-03-02	18612*	72.5	0.07±0.01 (core)	-
			0.09±0.02 (HST-1)	-
			0.04±0.02 (knot A)	-
2017-04-11	20034	13.1	-	-
2017-04-14	20035	13.1	0.08±0.06 (knot A)	-
2018-04-24	21076	9.0	-	-
2019-03-27	21457	14.1	-	-
2019-03-28	21458	12.8	-	-

Table 2: List of NuSTAR data analyzed in this study. For each ID, an upper ID is taken by Focal Plane Module-A (FPMA) and a lower is taken by FPMB.

Start date (YYYY-MM-DD)	Obs ID	exposure time (ksec)	RMS	RMS_{bgd}
2017-02-15	60201016002	50.3	0.09±0.08	-
			0.04±0.04	0.04±0.02
2017-04-11	90202052002	24.4	-	-
			0.04±0.04	-
2017-04-14	90202052004	22.5	-	-
			-	-
2018-04-24	60466002002	21.1	-	-
			-	-
2019-03-26	60502010002	23.6	-	-
			-	-
2019-03-28	60502010004	20.9	-	-
			-	-

Table 3: List of NuSTAR data analyzed in this study. For each ID, an upper ID is taken by Focal Plane Module-A (FPMA) and a lower is taken by FPMB.

Start date (YYYY-MM-DD)	Obs ID	exposure time (ksec)	RMS	RMS_{bgd}
2017-02-15	60201016002	50.3	0.09±0.08	-
			0.04±0.04	0.04±0.02
2017-04-11	90202052002	24.4	-	-
			0.04±0.04	-
2017-04-14	90202052004	22.5	-	-
			-	-
2018-04-24	60466002002	21.1	-	-
			-	-
2019-03-26	60502010002	23.6	-	-
			-	-
2019-03-28	60502010004	20.9	-	-
			-	-

XIS consists of three available CCDs in this observation, XIS0, XIS1, and XIS3. XIS0 and XIS3 are front-illuminated CCDs, wheareas XIS1 is a back-illuminated CCD. Therefore, the sensitivity of the low energy range of XIS1 is superior to XIS0 and XIS3 [5]. In each instrument, a circle with a radius of 3.0 arcmin was defined as the source region. The light curves of each CCD are created with `lcurve` command in an energy range of 3.0–10.0 keV with a time bin of 8400 s. Circles with a radius of 3.0 arcmin at 8.0 arcmin from the core were defined as background regions.

2.2 Spectral analysis

2.2.1 NuSTAR and Chandra

There are six observations taken by both NuSTAR and Chandra simultaneously. Following the method of [9], we performed simultaneous fitting of NuSTAR and Chandra spectra to obtain the photon index and flux of each component. In the simultaneous fitting, one NuSTAR spectrum and three Chandra spectra of the core, HST-1, and jet were fitted with the model of hot gas emission was considered for the NuSTAR spectrum, and each power-law model was considered for the NuSTAR spectrum and one Chandra spectrum of each component. Power-law parameters were common between NuSTAR and Chandra.

NuSTAR spectra were extracted in a circular region with a radius of 30 arcsec, and background regions were taken at 80–130 arcsec from M87. For Chandra spectra of each component, the source region of core and HST-1 were defined as a circle with a position specified in Figure 2 and a radius of 0.4 arcsec. For the background of core and HST-1 spectra, a half-circular band region at 2–4 arcsec was specified in the direction opposite to the jet (Figure 2). The jet area, including knots D and A, is defined as shown in Figure 2, and the background region was specified as 19.5 arcsec × 3 arcsec boxes on both sides of the jet. We created Chandra spectra with `specextract` command and binned the spectra so that 1 bin contained more than 20 photons. The spectral model for simultaneous fit consists of two temperature thermal plasma and three power-law models with Galactic absorption:

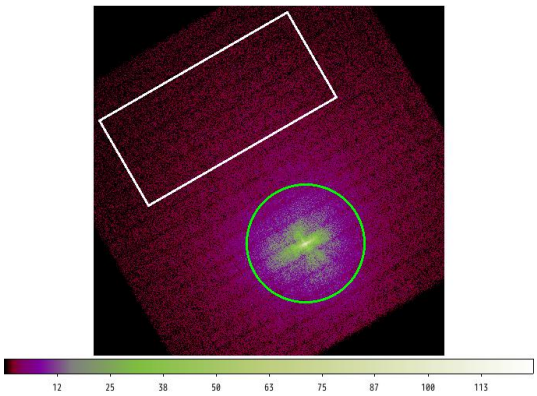

Figure 1: Extraction region of Suzaku spectra overlaid on the XIS1 image.The green circle with 3 arcmin is the source region, and the white box (5 arcmin×11 arcmin) is the background region.

`wabs*(vapec+vapec+pegpwrlw+pegpwrlw+pegpwrlw)` in `XSPEC`. The normalization of `vapec` was set to 0 for Chandra spectra, and `vapec` parameters for NuSTAR were fixed as described later. A column density of Galactic absorption was fixed to $1.94\times10^{20}\mathrm{cm}^{-2}$. Three `pegpwrlw` models represent emission from the core, HST-1, and jet. Thus, for each Chandra spectrum of the core, HST-1, and jet, only one `pegpwrlw` normalization was left free and other normalizations were set to 0. For these analyses, photon index and normalization were unified between NuSTAR and Chandra. Considering cross-calibration uncertainly between FPMA and FPMB of NuSTAR, we added a constant model.

2.3 Suzaku

Spectral of Suzaku/XIS was extracted for the source region with a radius of 3 arcmin (Figure 1). Response files were made by `xisarfgen` and`xisrmfgen` command.
We fitted the spectra in 1.0–10.0 keV with `wabs*(vapec+vapec+pegpwrlw)`. The metal abundances of H, C, and N were fixed to 1, and the abundance parameters of other metals are unified between the two `vapec` models. As a result, temperatures became 2.45 and 1.53 keV. The spectra were well fitted with a reduced χ square of χ^2/d.o.f = 1.25. Photon index became $\gamma = 2.38^{+0.07}_{-0.04}$ (2.0–10.0 keV), and the power-law flux became $2.71^{+0.18}_{-0.18}\times 10^{-11}$ erg cm^{-2} s^{-1}.

3. Result

To evaluate a short-term time variability, we calculated a RMS from X-ray light curves of each observation. RMS is defined as the following equation [6].

$$\mathrm{RMS} = \sqrt{\frac{\sum_i[(d_i-\bar{d})^2-e_i^2]}{N\bar{d}^2}} \tag{1}$$

Where d_i is a count rate of i-th data, N is the number of data points, $\bar{d}$ is an average, and e_i is a statistical error of d_i. Table 1 summarizes the RMS values of each observation. The RMS of observations with $\sum_i[(d_i-\bar{d})^2-e_i^2] < 0$ is not shown, indicating no variability. As a result,

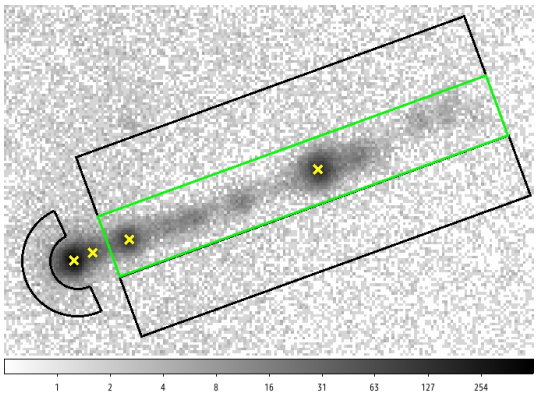

Figure 2: M87 X-ray image obtained via Chandra-ACIS (2019-3-27; ID18612). Crosses in the figure show positions of core, HST-1, knot D, and knot A from the left. The green box represents the jet region. The white half-circular band shows the background region of the core and HST-1 and the white boxes show the background region of the jet (including knots D and A) for spectral analysis.

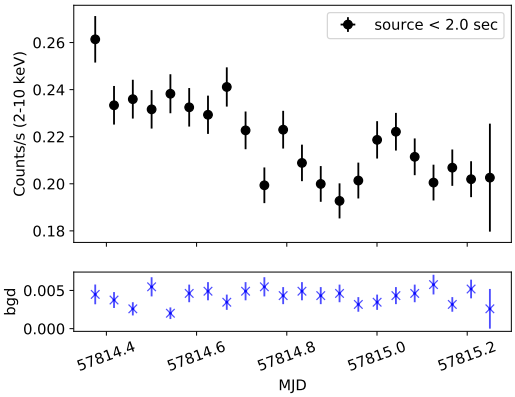

(a) Chandra core (2017-03-02)

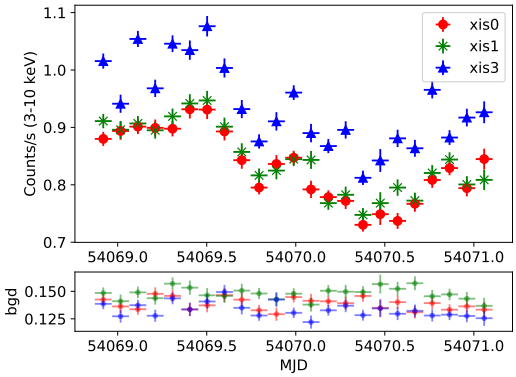

(b) Suzaku (2006-11-29)

some data showed significant variability. Figure 3(a) and 3(b) show light curves which estimated variabilities from the RMS.

Intraday variability is seen in Suzaku observation in 2006 (Fig.3(b)) and Chandra observation in 2017 (ID:18612, Fig.3(a)). For the Suzaku light curve, count rate changes by approximately 30% with a time scale of 0.3 days. There is a difference of count rates between XIS0 and XIS3, which is attributable to the off-axis observation [4]. The Chandra light curve of the core in 2017 showed approximately 40% variability with a time scale of 0.5 days. However, since the extraction region of Chandra data was as small as 2.0 arcsec, the fluctuation of the satellite attitude may cause a variability of the count rate. Therefore, we made light curves with different extraction radii of 0.4, 1.0, 2.0, and 4.0 arcsec to evaluate the systematic effects. From this analysis, RMS became 0.10±0.01, 0.09±0.01, 0.08±0.01, and 0.06±0.01, for 0.4, 1.0, 2.0, and 4.0 arcsec, respectively. The RMS decreased as the radius increased, but variability was significant, even for a large radius.

4. Discussion

The results obtained in this study are summarized below. First, the Suzaku observation in 2006 and the Chandra core observations in 2017 showed significant intraday X-ray variability. In the Suzaku light curve, the variability amplitude was approximately 30% with a time scale of about 0.3 days. For Chandra, the amplitude was approximately 40% with a time scale of 0.5 days. In 2006, the HST-1 was much brighter than the core in the X-ray band [10]. Moreover, in 2017 the core was brighter than the HST-1. The spectrum obtained by Suzaku in 2006 showed a steep photon index of $2.38^{+0.07}_{-0.04}$, and the core obtained by Chandra and NuSTAR in 2017 had a hard photon index of $1.96^{+0.05}_{-0.04}$. Minimum size $R_{\rm min}$ of emission region was estimated by X-ray variability time scale Δt as follows,

$$R_{\rm min} = \frac{c\Delta t \delta_D}{1+z} \tag{2}$$

where δ_D is a Doppler factor and z is a redshift. We found Δt ~0.3 day in 2006, and thus we obtain $R_{\rm min} \simeq 1.0\delta_D \times 10^{15}$ cm. Here, a central black hole mass was assumed to be $M_{\rm BH} = (6.5\pm0.7)\times 10^9$ $M_\odot$[3], The Schwartzschild radius is $R_s \sim 2.0 \times 10^{15}$cm. Thus, the size of the emission region was as compact as about $\sim R_{\rm s}$. Suzaku-XIS cannot resolve each component of the M87 jet, but knots D and A were quite fainter than the core and HST-1. In addition, X-ray spectra of knots D and A were reported to be soft with a photon index of 2.4-2.6, $\simeq$ 2.2, respectively [7] and thus it is difficult for the knots D and A to explain a rapid variability above 3.0 keV.

From the result of Chandra on November 13, 2006, a count rate ratio of HST-1 to the core was approximately about 4.45 [10]. If the variability was only due to the core, A core count rate of the core must vary with an amplitude $\sim$ 260%. Such an extreme large amplitude of variability has never been observed for the M87 core, and thus it is unlikely. The X-ray spectrum in 2006 was steep with a photon index of 2.38. [2] showed that X-ray emission observed by Suzaku could be explained by a high-energy tail of synchrotron, based on the spectral energy distribution (SED) modeling and thus concluded that HST-1 is likely the origin of TeV gamma-rays. These results implied that X-ray intraday variability in 2006 observed by Suzaku-XIS can be explained by synchrotron radiation from HST-1.

Assuming that X-ray decay was due to electron cooling, we could estimate a magnetic field strength. The cooling time scale was expressed by the following equation from [8]

$$\tau_s = 3.2 \times 10^4 \times B^{-3/2} \times E_{\rm ph}^{-1/2} \times \delta^{-1/2} ({\rm s}) \tag{3}$$

where, τ_s is the decay time scale, B is the strength of magnetic field, $E_{\rm ph}$ is the photon energy in the observer frame, and δ is the Doppler factor. Using a decay time scale of 0.3 days, and $E_{\rm ph}$ = 6500 eV, and a Doppler factor δ, the magnetic field became $B = 1.94\delta^{1/3}$ mG. Using the estimated magnetic field, electron energy emitting synchrotron X-ray emission should be $1.1 \times 10^8 \gamma^{-1} \delta^{-1/3}$ TeV, and thus particle acceleration up to TeV was indicated to occur in the HST-1.

How about an X-ray variability of the core with a time scale Δt~0.5 days in 2017 is? VERITAS observations in 2008 showed that, the X-ray flux of the core simultaneously varied with TeV gamma-ray flux, suggesting that the core X-ray emission originated from the jet as well as TeV gamma-ray [1]. Therefore, the 2017 variability could be due to jet emission at the core. The power-law photon index of the core X-ray spectrum in 2017 is $1.96^{+0.05}_{-0.04}$, which could be the inverse Compton scattering component rather than synchrotron radiation if it comes from the jet.

In the six NuSTAR and Chandra observations in 2017-2019, the flux of the core was high by a factor of 2.5 in only one observation of April 2018. The core emission in this period is considered as jet inverse Compton or ADAF radiation rather than jet synchrotron radiation, as discussed above. Since the variability time scale is just constrained to be longer than 1 day, we cannot discuss the origin of variability anymore.

References

[1] Acciari, V. A., Beilicke, M., Blaylock, G., & Bradbury, S. M. 2008, The Astrophysical Journal, 679, 397, doi: 10.1086/587458

[2] de Jong, S., Beckmann, V., Soldi, S., Tramacere, A., & Gros, A. 2015, Monthly Notices of the Royal Astronomical Society, 450, 4333, doi: 10.1093/mnras/stv927

[3] Event Horizon Telescope. 2019, The Astrophysical Journal Letters, 875, L6, doi: 10.3847/2041-8213/ab1141

[4] JAXA/ISAS, & NASA/GFSC. 2015, The Suzaku Technical Description, 6.X-Ray Telescopes (XRT). https://heasarc.gsfc.nasa.gov/docs/suzaku/prop_tools/suzaku_td/node9.html#fig:2-10keV

[5] Koyama, K., Tsunemi, H., & Dotani. 2007, Publications of the Astronomical Society of Japan, 59, S23, doi: 10.109/pasj/59.sp1.S23

[6] Shirai, H., Fukazawa, Y., Sasada, M., Ohno, M., & Yonetoku. 2008, Publications of the Astronomical Society of Japan, 60, S263, doi: 10.1093/pasj/60.sp1.S263

[7] Sun, Xiao-Na, Yang, Rui-Zhi, Rieger, Frank M., Liu, Ruo-Yu, & Aharonian, Felix. 2018, Astronomy and Astrophysics, 612, A106, doi: 10.1051/0004-6361/201731716

[8] Tashiro, M., Makishima, K., Ohashi, T., et al. 1995, PASJ, 47, 131

[9] Wong, K.-W., Nemmen, R. S., Irwin, J. A., & Lin, D. 2017, The Astrophysical Journal, 849, L17

[10] Yang, S., Yan, D., Dai, B., et al. 2019, Monthly Notices of the Royal Astronomical Society, 489, 2685–2693, doi: 10.1093/mnras/stz2302